Acta Crystallographica Section B
Structural Science, Crystal Engineering and Materials
ISSN 2052-5206

The ecstasy and the agony; compression studies of 3,4-methylenedioxymethamphetamine (MDMA)

Lauren E. Connor,[a] Amit Delori,[a] Ian B. Hutchison,[a] Niamh Nic Daeid,[b] Oliver B. Sutcliffe[c] and Iain D. H. Oswald[a]*

[a]Strathclyde Institute of Pharmacy and Biomedical Sciences, University of Strathclyde, 161 Cathedral Street, Glasgow G4 0RE, Scotland, [b]Centre for Anatomy and Human Identification, University of Dundee, College of Life Sciences, Dow Street, Dundee DD1 5EH, Scotland, and [c]School of Science and the Environment, Manchester Metropolitan University, Chester Street, Manchester M1 5GD, England

Correspondence e-mail: iain.oswald@strath.ac.uk

Received 27 October 2014
Accepted 1 December 2014

MDMA (3,4-methylenedioxymethamphetamine) is a Class A substance that is usually found in a tableted form. It is only observed in one orthorhombic polymorph under ambient conditions. It shows slight positional disorder around the methlyenedioxy ring which persists during compression up to 6.66 GPa. The crystal quality deteriorates above 6.66 GPa where the hydrostatic limit of the pressure-transmitting medium is exceeded. The structure undergoes anisotropic compression with the *a*-axis compressing the greatest (12% *cf.* 4 and 10% for the *b*- and *c*-axes, respectively). This is due to the pattern of the hydrogen bonding which acts like a spring and allows the compression along this direction.

1. Introduction

3,4-Methylenedioxymethylamphetamine hydrochloride (MDMA) is a synthetic entactogen, which is structurally similar to methylamphetamine (MA), and acts as a CNS stimulant, producing mood enhancement, increased energy and other empathetic effects by increasing the intra-synaptic concentrations of key neurotransmitters (serotonin, dopamine and norepinephrine; Fig. 1; Buckley, 2012; Pentney, 2001). MDMA was first synthesized (and patented) by Merck in 1912 as a potential appetite suppressant, however, the company never marketed it as such. Over the next 70 years, a number of researchers evaluated the psychedelic properties of MDMA in an attempt to harness its legitimate potential in psychotherapy – with little success (Colado *et al.*, 2007). In the 1970s and 1980s the substance surfaced on the recreational drug scene and its widespread abuse led many countries to prohibit the possession, supply and manufacture of MDMA. Currently, in the UK, MDMA (or 'ecstasy') is controlled as a Class A, Schedule 1 substance due to its illicit use as recreational drug, and its implication in a number of highly publicized fatalities (De Letter *et al.*, 2010; Turillazzi *et al.*, 2010; Verschraagen *et al.*, 2007). It is usually found in tableted form with each batch being stamped with a particular motif, *e.g.* a Mitsubishi logo, smiley faces or letters. The tableting procedure subjects the material to elevated pressures in which conversion to other polymorphs may occur.

We have previously investigated illicit materials under a variety of conditions including high pressure to investigate whether polymorphism of these materials exists (Delori *et al.*, 2014; Satthaphut *et al.*, 2014). Pharmaceutical companies subject formulations to rigorous scrutiny to ensure that their pharmaceutical products are stable and are present in only one form under certain manufacturing conditions (do Nascimento *et al.*, 2010); this is not the case in clandestine laboratories. Polymorphism in these materials has received little or no attention. Lee *et al.* (2000) investigated MDMA·HCl and

some related compounds *via* ^{13}C NMR and found that there were chemical shifts induced in the racemic MDMA·HCl when mixed with lactose and suggested interaction between MDMA·HCl and lactose. They postulated that polymorphism existed in this system, however, Morimoto *et al.* (1998) and Zapata-Torres *et al.* (2008) are the only groups to have investigated MDMA·HCl and the monohydrate, respectively. The latter observation of a hydrate may have been what Lee *et al.* had detected. Nevertheless, given that polymorphism has an impact on physical properties, such as solubility and bioavailability, it could be suggested that different clandestine drug laboratories manufacture different solid-state forms of MDMA·HCl particularly in the final tableting stage. The pressure on tableting, albeit not as great as most high-pressure studies (up to 600 MPa, 0.6 GPa), may convert ecstasy into different polymorphic forms as observed in many molecular complexes (Fabbiani *et al.*, 2010; Patyk *et al.*, 2012; Tumanov *et al.*, 2010; Funnell *et al.*, 2011; Millar *et al.*, 2010; Oswald & Pulham, 2008). Herein we report the compression study of ecstasy to ∼7 GPa highlighting the structural changes that occur on compression.

2. Experimental

2.1. Recrystallization

Racemic MDMA·HCl was prepared in house *via* the sodium borohydride method (Buchanan *et al.*, 2008), and isopropyl alcohol (IPA) and petroleum ether were supplied by Sigma-Aldrich. A crude sample of MDMA·HCl was recrystallized from IPA. Crude MDMA·HCl (20 mg, 0.087 mmol) was added to a vial followed by 2.5 ml of IPA. The vial was heated gently for 2 min before leaving the vials to return to room temperature without caps. Colourless single crystals of diffraction quality formed from this solution.

2.2. Generation of high pressure

A Merrill–Bassett diamond–anvil cell adapted to fit Boehler Almax backing discs and diamonds was used to generate the pressure in the cell (Moggach *et al.*, 2008). A tungsten foil was indented to a thickness of 100 µm and a hole (300 µm) drilled in the gasket using an Almax Easylab Microdriller. A single crystal of MDMA·HCl, which was recrystallized from 2-propanol, was loaded into the cell together with a ruby sphere (for pressure calibration) and petroleum ether (40:60) which served as the pressure-transmitting medium (Piermarini *et al.*, 1975; Tateiwa & Haga, 2009). Three crystals were used to complete the high-pressure datasets due to large pressure jumps between datasets in the initial compression study. Furthermore, the crystal undergoes a sharp deterioration in the diffraction above ∼7 GPa so two further studies were made to gain a more precise pressure at which the transition occurs.

2.3. Single-crystal X-ray diffraction

2.3.1. Ambient-pressure data collection and refinement. X-ray diffraction intensities were collected using a Bruker APEX II diffractometer with an Incotec IμS microsource (λ = 0.71073 Å). Data were reduced using *SAINT* as incorporated in the *APEX*II (Bruker, 2010) suite of programs. An absorption correction was applied using *SADABS* (Sheldrick, 2008). The crystal structure at ambient pressure was solved by direct methods (*SIR*92; Altomare *et al.*, 1994) and refined using the *CRYSTALS* refinement package (Betteridge *et al.*, 2003). Distance restraints were used to ensure the geometry of the methylenedioxy ring was chemically reasonable using mean values for similar structures observed in the Cambridge Structural Database *via* the Mogul search (Allen, 2002; Bruno *et al.*, 2004). The disordered model was constructed by splitting the O atoms that possessed elongated thermal parameters and restraining the distances as above. The different orientations were competitively refined. Vibrational and thermal similarity restraints were applied over all atoms. The H atoms of the N1 were refined with restraints as implemented in Version 14.61 of *CRYSTALS*.

2.3.2. High-pressure data collections and refinements. The data were collected as above but the treatment of the data was slightly modified. The data were reduced using a dynamic masking procedure as outlined by Dawson *et al.* (2004).

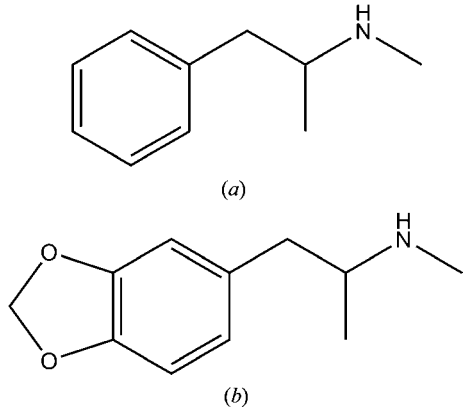

Figure 1
The chemical structures of (*a*) MA and (*b*) MDMA.

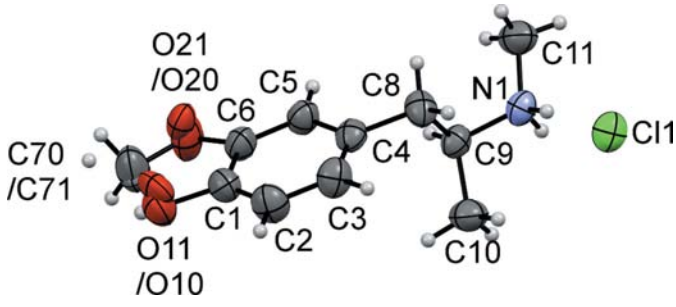

Figure 2
A displacement ellipsoid plot of MDMA·HCl at ambient pressure showing the numbering scheme used. The disordered atoms are labelled with 0 and 1 to represent the different orientations, *i.e.* O10, C70 and O20 are one orientation and O11, C71 and O21 are the other orientation. Colour scheme for atoms: blue, nitrogen; grey, carbon; red, oxygen; green, chloride; white, hydrogen.

Table 1
For all structures: $C_{11}H_{16}NO_2{\cdot}Cl$, M_r = 229.71, orthorhombic, $Pca2_1$, Z = 4. Experiments were carried out at 293 K with Mo $K\alpha$ radiation using a Bruker Kappa APEXII diffractometer. Absorption was corrected for by multi-scan methods, *SADABS* (Sheldrick, 2008). H atoms were treated by a mixture of independent and constrained refinement. Datasets (1), (2) and (7) were collected on three different crystals, however, the datasets (3)–(6) were collected on the same crystal.

	(1)	(2)	(3)	(4)
Crystal data				
Pressure (GPa)	Ambient	1.14	2.2	3.84
a, b, c (Å)	9.4272 (2), 7.0774 (2), 18.2519 (4)	9.1478 (3), 6.9826 (3), 17.6799 (4)	8.8661 (5), 6.9379 (4), 17.120 (3)	8.4895 (2), 6.8759 (2), 16.6225 (14)
V (Å^3)	1217.77 (3)	1129.31 (3)	1053.08 (17)	970.30 (8)
μ (mm^{-1})	0.30	0.32	0.34	0.37
Crystal size (mm)	0.35 × 0.22 × 0.10	0.20 × 0.10 × 0.05	0.20 × 0.10 × 0.05	0.20 × 0.10 × 0.05
Data collection				
T_{min}, T_{max}	0.83, 0.97	0.87, 0.98	0.87, 0.98	0.89, 0.96
No. of measured, independent and observed [$I > 2.0\sigma(I)$] reflections	26 105, 2636, 2603	5069, 1027, 977	4833, 572, 530	4431, 522, 498
R_{int}	0.033	0.033	0.038	0.032
θ_{max} (°)	27.1	23.3	23.3	23.2
$(\sin\theta/\lambda)_{max}$ (Å^{-1})	0.641	0.557	0.556	0.555
Refinement				
$R[F^2 > 2\sigma(F^2)]$, $wR(F^2)$, S	0.027, 0.080, 1.01	0.035, 0.081, 1.04	0.031, 0.071, 1.03	0.027, 0.062, 0.97
No. of reflections	2628	1023	567	518
No. of parameters	171	86	86	86
No. of restraints	158	56	56	56
$\Delta\rho_{max}$, $\Delta\rho_{min}$ (e Å^{-3})	0.18, −0.10	0.61, −0.57	0.23, −0.22	0.14, −0.12
Absolute structure	Flack (1983), 1254 Friedel pairs	Flack (1983), 355 Friedel pairs	Flack (1983), 455 Friedel pairs	Flack (1983), 50 Friedel pairs
Absolute structure parameter	0.04 (5)	0.07 (11)	0.19 (16)	−0.02 (15)

	(5)	(6)	(7)
Crystal data			
Pressure (GPa)	4.42	5.24	5.98
a, b, c (Å)	8.4043 (2), 6.8578 (2), 16.5271 (12)	8.3242 (4), 6.8403 (3), 16.447 (2)	8.3325 (8), 6.814 (2), 16.4416 (16)
V (Å^3)	952.54 (7)	936.48 (13)	933.50 (9)
μ (mm^{-1})	0.38	0.38	0.39
Crystal size (mm)	0.20 × 0.10 × 0.05	0.20 × 0.10 × 0.05	0.20 × 0.10 × 0.05
Data collection			
T_{min}, T_{max}	0.91, 0.96	0.92, 0.96	0.77, 0.98
No. of measured, independent and observed [$I > 2.0\sigma(I)$] reflections	4206, 493, 459	4137, 486, 441	2043, 510, 472
R_{int}	0.033	0.036	0.042
θ_{max} (°)	23.2	23.3	23.3
$(\sin\theta/\lambda)_{max}$ (Å^{-1})	0.555	0.557	0.556
Refinement			
$R[F^2 > 2\sigma(F^2)]$, $wR(F^2)$, S	0.022, 0.055, 1.02	0.026, 0.058, 1.02	0.043, 0.106, 1.01
No. of reflections	489	478	507
No. of parameters	86	86	86
No. of restraints	56	56	56
$\Delta\rho_{max}$, $\Delta\rho_{min}$ (e Å^{-3})	0.20, −0.22	0.22, −0.21	0.47, −0.50
Absolute structure	Flack (1983), 29 Friedel pairs	Flack (1983), 7 Friedel pairs	Flack (1983), 24 Friedel pairs
Absolute structure parameter	0.04 (13)	−0.10 (14)	0.21 (19)

Computer programs: *APEX*II (Bruker, 2010), *SIR92* (Altomare *et al.*, 1994), *CRYSTALS* (Betteridge *et al.*, 2003).

Corrections were applied using *Shade* (Parsons, 2004) and the absorption corrections applied using *SADABS* (Sheldrick, 2008). The starting point for the initial pressure was the ambient pressure model and each subsequent refinement started with the refined model from the previous pressure. Due to the low completeness of the data only the chloride ion was refined anisotropically. Similar restraints were applied to the high-pressure datasets. The numbering scheme for this study is found in Fig. 2 and the full crystallographic information can be found in Table 1.

Other programs used for analysis and figures were *PLATON* (Spek, 2003), Materials *Mercury* (Macrae *et al.*, 2008), *OriginPro* (OriginLab, http://originlab.com).

2.3.3. High-pressure powder diffraction. The DAC was prepared as above but loaded with a powder of MDMA·HCl, a ruby and petroleum ether as the pressure-transmitting

Table 2
Hydrogen-bonding parameters (Å, °) at each pressure.

Pressure (GPa)		*D*—H	H···*A*	*D*···*A*	*D*—H···*A*
Ambient	H11—Cl1	0.914 (15)	2.229 (15)	3.1392 (12)	173.3 (15)
	H12—Cl1	0.907 (15)	2.207 (15)	3.0961 (13)	166.7 (13)
1.14	H11—Cl1	0.90 (2)	2.25 (2)	3.123 (4)	166 (2)
	H12—Cl1	0.87 (2)	2.256 (18)	3.072 (4)	156 (2)
2.2	H11—Cl1	0.91 (2)	2.21 (2)	3.073 (4)	159 (2)
	H12—Cl1	0.89 (2)	2.217 (18)	3.053 (4)	157 (2)
3.84	H11—Cl1	0.91 (2)	2.20 (2)	3.014 (3)	150 (2)
	H12—Cl1	0.874 (18)	2.196 (17)	3.016 (4)	156 (2)
4.42	H11—Cl1	0.91 (2)	2.19 (2)	2.998 (3)	148 (2)
	H12—Cl1	0.864 (18)	2.198 (17)	3.013 (4)	157 (2)
5.25	H11—Cl1	0.91 (2)	2.16 (2)	2.984 (4)	149 (2)
	H12—Cl1	0.874 (18)	2.200 (17)	3.009 (4)	154.1 (19)
5.98	H11—Cl1	0.88 (2)	2.2 (3)	3.003 (13)	152 (2)
	H12—Cl1	0.89 (2)	2.19 (3)	3.005 (5)	153 (3)

medium. The cell was centred as per the single-crystal experiment before a 10 min exposure was taken. The cell was rotated by 20° during the data collection. The image was processed and the powder pattern integrated using the Pilot module within the *APEX*II suite of programs. A Pawley fit was performed using *TOPAS-Academic* (Coelho, 2012).

2.4. Cambridge Structural database

A fragment based on the backbone of MDMA (C_7O_2) was used as a query to search the Cambridge Structural Database, Version 5.35 (plus all updates) *via ConQuest*, 1.16 (Bruno *et al.*, 2002). This fragment contained no substituents and there were no restrictions applied to the search. The torsional angles around the methylenedioxy group were highlighted for retrieval. 1424 structures were found with 1952 fragments observed.

For the $NH_2^+\cdots Cl^-$ search a simple secondary ammonium group was chosen with no substituents on the neighbouring C atoms. Only organics with three-dimensional coordinates determined, no polymers, errors or disorder compounds were chosen for the search.

3. Results and discussion

3.1. Ambient-pressure structure

MDMA·HCl recrystallizes in one polymorphic form under ambient conditions. It crystallizes in orthorhombic $Pca2_1$ with one formula unit in the asymmetric unit. We have attempted to recrystallize the sample from a range of solvents, but it only had sufficient solubility in IPA and water. Crystals from IPA were of good enough quality for diffraction. The data are consistent with previous literature, but we observe elongated anisotropic parameters associated with the methylenedioxy ring O atoms suggesting that the ring system is disordered over two positions (Fig. 2). Morimoto *et al.* (1998) did not model this disorder but the *ORTEP* plot from their paper also shows slightly elongated thermal parameters. One factor to note is that their data collection was made at 161 K, whereas the present collection was made at 293 K and so the disorder present in their structure may have been less apparent. The monohydrate structure also reveals some disordered component around one of the methlyenedioxy O atoms (Zapata-Torres *et al.*, 2008).

The conformation of MDMA·HCl resembles one of the lowest energy conformers around the tail group (assuming *R* and *S* conformations are equally low in energy; Lee *et al.*, 2000). The angle between the least-squares plane of the phenyl ring and that of the methylenedioxy group is observed to be ~ 10 and $\sim 27°$ for the different conformations in our ambient-pressure structure. These compare favourably with similar structures found in the CSD (0–25°). The rest of the molecule shows that the tail group of the cation lies almost perpendicular to the least-squares plane of the ring system and that hydrogen bonds are formed between the NH_2^+ group and the Cl^- ion [$N\cdots Cl^- = 3.0961$ (13) and 3.1392 (12) Å; Table 2]. The chains of molecules are observed to run parallel to the *a*-axis with the cations lying on one side of the chain forming a cup when projected along this axis. Symmetry-related chains *via* the 2_1-screw axis pack closely along the *c*-axis (Fig. 3). Other symmetry-related chains $(\frac{1}{2}-x, 1+y, \frac{1}{2}+z)$ show close interaction between the methylene group (C70/71) with the chloride anion and between the O10/11 and the methyl group (C11) of a neighbouring molecule $(1-x, -y, -\frac{1}{2}+z)$.

3.2. Compression studies

The crystal structure shows a smooth anisotropic compression with the *a*-axis reducing by 12%, the *b*-axis reducing by 4% and the *c*-axis reducing by 10% up to a pressure of 6.66 GPa (Fig. 4). Whilst no structural information suitable for publication could be elucidated from the data at 6.66 GPa, the unit-cell parameters, space-group symmetry and

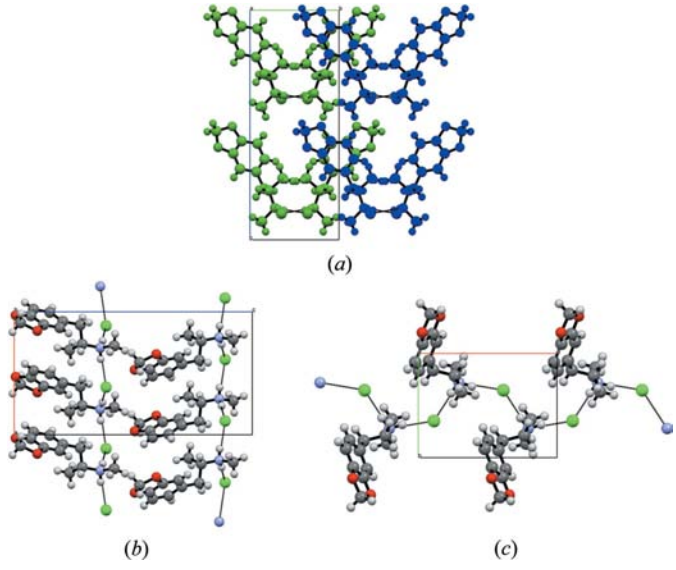

Figure 3
A view of the structure of MDMA·HCl along the (*a*) *a*-axis (neighbouring chains along the *b*-axis are coloured green and blue); (*b*) *b*-axis; (*c*) *c*-axis. An ordered model was used for clarity. For (*b*) and (*c*) the colour scheme is the same as in Fig. 2.

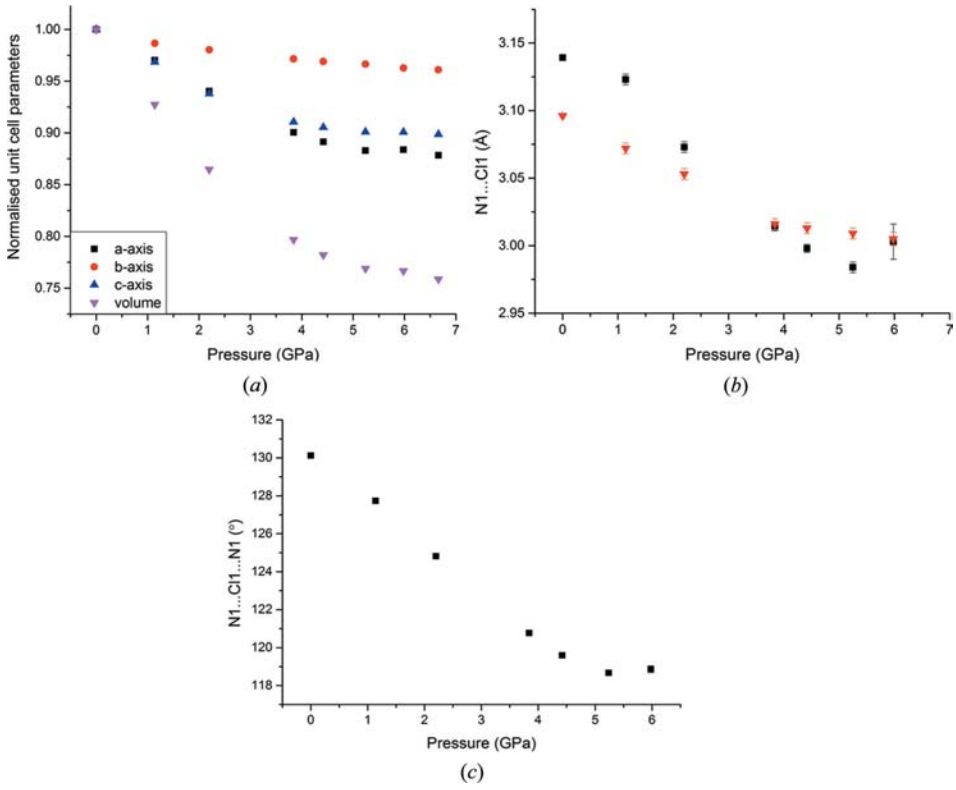

Figure 4
(*a*) The normalized unit-cell parameters and volume as a function of pressure for MDMA·HCl, (*b*) hydrogen bond lengths and (*c*) hydrogen bonding angles as observed in MDMA·HCl as a function of pressure.

initial refinement show that the ambient-pressure polymorph is still present [R factor 0.093 with 232 reflections, $F^2 > 2\sigma(F^2)$].

On increasing pressure the hydrogen-bonding distances for N1···Cl1 steadily decrease from 3.0961 (13) and 3.1392 (12) Å to 3.005 (5) and 3.003 (13) Å, respectively (Fig. 4). This accounts for a 4.3 and 2.9% reduction in the hydrogen bond lengths over 5.98 GPa, which is reasonable for this type of system (Fig. 5). A search of the CSD shows that the hydrogen bond lengths at ambient pressure are comparable with similar types of interactions observed in a wide set of secondary ammonium complexes with chloride ions as counterions. The mean for these types of interactions is 3.126 Å from 2047 counts (837 hits) (Fig. 5). On compression both of the hydrogen bonds are reduced to ∼ 3 Å, which is at the lower end of the histogram for these types of interactions; in fact, one of the interactions falls below 3 Å before increasing in length again at 5.98 GPa. There are a number of compounds with extremely short bonds [CAVVUQ02, 2.547 Å (Sysko & Allen, 1993); IWOCIH, 2.6750 Å (Wei *et al.*, 2010); XAHHAR, 2.7670 Å (Das *et al.*, 2010)] that have large molecular groups whose packing requirements need to be satisfied ahead of the hydrogen bonding; XAHHAR is an inclusion complex where the Cl^- is enclosed in the macrocycle.

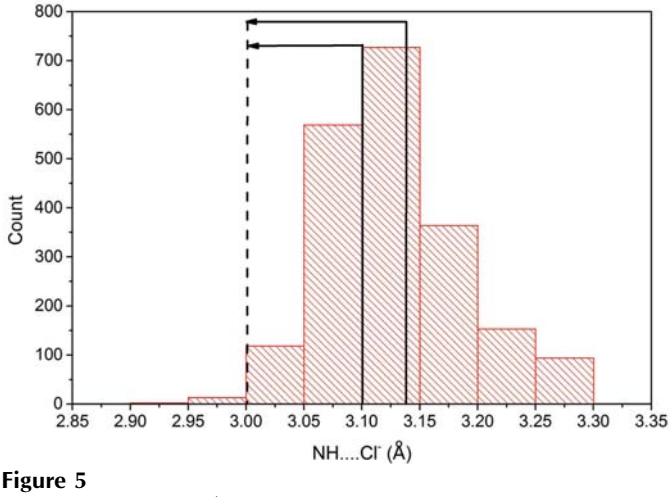

Figure 5
A histogram of $NH_2^+\cdots Cl^-$ distances observed in the CSD. The experimentally observed hydrogen bond lengths at ambient (solid) and 5.98 GPa (dotted). Compounds with hydrogen bonds shorter than 2.85 Å have been excluded for clarity of the main histogram.

Beyond 7 GPa, which is beyond the hydrostatic limit for the pressure-transmitting medium, the diffraction pattern deteriorates considerably (Figs. 6*a* and *b*). A powder pattern of a sample at 7.27 GPa was collected on our APEXII diffractometer for 10 min. Whilst the intensity is not particularly strong, we were able to estimate the cell parameters using the previous data points and input these into *TOPAS-Academic* and perform a Pawley fit on the data (Fig. 6*c*). The fit is reasonable, considering the strength of the data, and is sufficient to conclude that the deterioration was due to the hydrostatic limit of the pressure-transmitting medium and not through a reconstructive phase transition. A closer inspection of the unit-cell axes shows that the compression along both the *a*- and *c*-axes have reached a minimum, whilst the *b*-axis is still compressing (at 6.66 GPa) towards a minimum value. The unit-cell parameters from the Pawley refinement at 7.27 GPa are $a = 8.3003$, $b = 6.7649$, $c = 16.418$ Å with a cell volume of 921.92 Å^3, but these parameters are reported with caution. In this instance the phase remains intact, but the hydrogen-bond distances have compressed to a minimum suggesting that a phase transition may be imminent. Other research has highlighted that hydrogen bonds can be compressed to a minimum value as observed in the CSD before a change of phase occurs to relieve the repulsive forces (Wood *et al.*, 2008).

As well as the change in the hydrogen bond distance there is a substantial alteration in the N···Cl···N angle of the

hydrogen-bonded chain. Fig. 3(*c*) is a view perpendicular to the hydrogen-bonded chain, where one can observe the sinusoidal pattern of the bonding. As pressure is applied the NH···Cl distances decrease but so does the N···Cl···N angle from ∼ 130 to 118°. One can use the analogy of a spring which is being compressed allowing for the largest compression along the *a*-axis; a more linear hydrogen-bonding arrangement would not be so compressible. Void analysis of the structure shows that there are voids located in the same plane as the hydrogen-bonded motif (Fig. 7, circled). These voids reduce substantially on compression largely due to the compression of the hydrogen-bonded chain along this direction. From the refined data, the parameters associated with the hydrogen bonding are compressed to a minimum which may signify that a phase transition may be imminent.

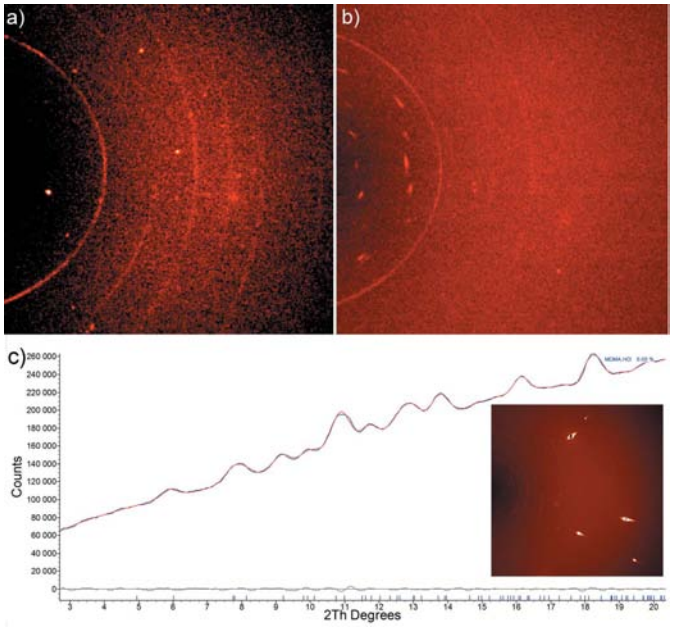

Figure 6
The diffraction patterns from the same crystal at (*a*) 5.24 GPa, (*b*) 7.1 GPa and (*c*) powder at 7.27 GPa. The Pawley fit using the diffraction pattern collected on our APEXII diffractometer using the *Pilot* module in *APEX*II software.

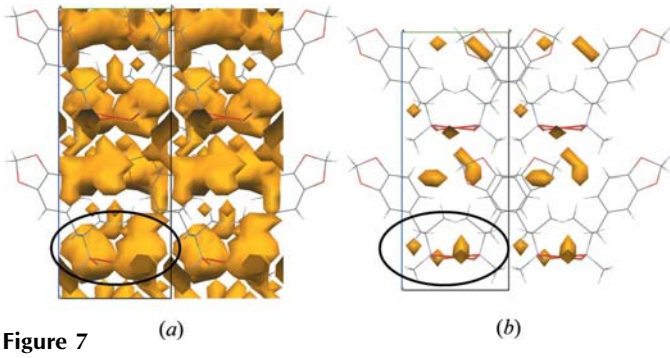

Figure 7
View down the *a*-axis of the void space of MDMA·HCl at (*a*) ambient pressure and (*b*) 5.98 GPa calculated with *Mercury* using a probe radius of 0.4 Å and a grid spacing of 0.7 Å. The circled area highlights the void space in one of the hydrogen-bonded chains.

As described for the ambient pressure structure the hydrogen-bonded chains stack along the *c*-direction. This axis is almost as compressible as the *a*-axis and this can be attributed to the lack of directional forces in this direction. Again, the voids in this direction are reduced considerably as pressure is applied. A further consequence of the compression along this direction is that, due to the orientation of the cations with respect to the *c*-axis, the 'cup' shape as described earlier flattens which has an impact on the length of the *b*-axis. There have been reports of materials showing negative compressibility in wine-rack-type structures under high-pressure conditions. This observation is intuitive if the molecules are aligned at an angle to the principal strain axes as compression along one axis means that another is elongated (Cairns *et al.*, 2013). Whilst this structure does not show a negative compressibility it does show that the compressibility of the *b*-axis is significantly reduced compared with the other two axes (4% *cf.* 10 and 12% from 0 to 5.98 GPa) and this can, in part, be attributed to the molecular orientation becoming more parallel to the *b*-axis. Further structural features that will contribute to this are the lack of voids between neighbouring chains along the *b*-axis. In total, the void space is reduced from 9% of the unit-cell volume to 0.6%.

4. Conclusions

Despite our initial idea that polymorphism of MDMA·HCl may exist with pressure, this investigation has shown that the single-crystal remains in the same phase from ambient pressure to 6.66. GPa. Beyond 7 GPa the diffraction pattern deteriorates sharply which can be attributed to the hydrostatic limit of the pressure-transmitting medium, but the same phase is still present. The sinusoidal hydrogen-bonding pattern permits the greatest compression of the structure to be along the direction of the hydrogen bonds. This is possible due to both a decrease in the bond lengths but also through a change in the N···Cl···N angle of the hydrogen bond. The orientation of the cation in the unit cell also impacts on the rate of compressibility of the *b*-axis compared with the *a*- and *c*-axes. The compression along the *c*-axis pushes the cation towards a more parallel orientation with respect to the *b*-axis.

The authors would like to acknowledge Dr Hilary Buchanan for preparation of the MDMA and Strathclyde Institute of Pharmacy and Biomedical Sciences for funding.

References

Allen, F. H. (2002). *Acta Cryst.* B**58**, 380–388.
Altomare, A., Cascarano, G., Giacovazzo, C., Guagliardi, A., Burla, M. C., Polidori, G. & Camalli, M. (1994). *J. Appl. Cryst.* **27**, 435.
Betteridge, P. W., Carruthers, J. R., Cooper, R. I., Prout, K. & Watkin, D. J. (2003). *J. Appl. Cryst.* **36**, 1487.
Bruno, I. J., Cole, J. C., Edgington, P. R., Kessler, M., Macrae, C. F., McCabe, P., Pearson, J. & Taylor, R. (2002). *Acta Cryst.* B**58**, 389–397.
Bruno, I. J., Cole, J. C., Kessler, M., Luo, J., Motherwell, W. D. S., Purkis, L. H., Smith, B. R., Taylor, R., Cooper, R. I., Harris, S. E. & Orpen, A. G. (2004). *J. Chem. Inf. Comput. Sci.* **44**, 2133–2144.

Bruker (2010). *APEXII* and *SAINT*. Bruker AXS Inc., Madison, Wisconsin, USA.
Buchanan, H. A. S., Daéid, N. N., Meier-Augenstein, W., Kemp, H. F., Kerr, W. J. & Middleditch, M. (2008). *Anal. Chem.* **80**, 3350–3356.
Buckley, N. A. (2012). *Medical Toxicology of Drug Abuse: Synthesized Chemicals and Psychoactive Plants.* Hoboken, NJ: John Wiley and Sons Inc.
Cairns, A. B., Catafesta, J., Levelut, C., Rouquette, J., van der Lee, A., Peters, L., Thompson, A. L., Dmitriev, V., Haines, J. & Goodwin, A. L. (2013). *Nat. Mater.* **12**, 212–216.
Coelho, A. (2012). *TOPAS-Academic*, Version 5. Coelho Software, Brisbane, Australia.
Colado, I. M., O'Shea, E. & Green, R. A. (2007). *Handbook of Contemporary Neuropharmacology*, edited by D. R. Sibley. New York: Wiley.
Das, M. C., Ghosh, S. K., Sen, S. & Bharadwaj, P. K. (2010). *CrystEngComm*, **12**, 2967–2974.
Dawson, A., Allan, D. R., Parsons, S. & Ruf, M. (2004). *J. Appl. Cryst.* **37**, 410–416.
De Letter, A., Stove, C. P., Lambert, W. E. & Piette, W. (2010). *Curr. Pharm. Biotech.* **11**, 453–459.
Delori, A., Maclure, P., Bhardwaj, R. M., Johnston, A., Florence, A. J., Sutcliffe, O. B. & Oswald, I. D. H. (2014). *CrystEngComm*, **16**, 5827–5831.
Fabbiani, F. P. A., Buth, G., Dittrich, B. & Sowa, H. (2010). *CrystEngComm*, **12**, 2541–2550.
Flack, H. D. (1983). *Acta Cryst.* A**39**, 876–881.
Funnell, N. P., Marshall, W. G. & Parsons, S. (2011). *CrystEngComm*, **13**, 5841–5848.
Lee, G. S. H., Taylor, R. C., Dawson, M., Kannangara, G. S. K. & Wilson, M. A. (2000). *Solid State Nucl. Magn. Reson.* **16**, 225–237.
Macrae, C. F., Bruno, I. J., Chisholm, J. A., Edgington, P. R., McCabe, P., Pidcock, E., Rodriguez-Monge, L., Taylor, R., van de Streek, J. & Wood, P. A. (2008). *J. Appl. Cryst.* **41**, 466–470.
Millar, D. I. A., Oswald, I. D. H., Barry, C., Francis, D. J., Marshall, W. G., Pulham, C. R. & Cumming, A. S. (2010). *Chem. Commun.* **46**, 5662–5664.
Moggach, S. A., Allan, D. R., Parsons, S. & Warren, J. E. (2008). *J. Appl. Cryst.* **41**, 249–251.
Morimoto, B. H., Lovell, S. & Kahr, B. (1998). *Acta Cryst.* C**54**, 229–231.
Nascimento, T. G. do, Basílio Júnior, I. D., Macêdo, R. O., Moura, E. A., Dornelas, C. B., Bernardo, V. B., Rocha, V. N. & Nóvak, C. (2010). *J. Therm. Anal. Calorim.* **102**, 269–275.
Oswald, I. D. H. & Pulham, C. R. (2008). *CrystEngComm*, **10**, 1114–1116.
Parsons, S. (2004). *Shade*. University of Edinburgh.
Patyk, E., Skumiel, J., Podsiadło, M. & Katrusiak, A. (2012). *Angew. Chem. Int. Ed.* **51**, 2146–2150.
Pentney, A. R. (2001). *J. Psychoactive Drugs*, **33**, 213–221.
Piermarini, G. J., Block, S., Barnett, J. D. & Forman, R. A. (1975). *J. Appl. Phys.* **46**, 2774–2780.
Satthaphut, N., Sutcliffe, O. B. & Oswald, I. D. H. (2014). *Z. Kristallogr.* **229**, 101–111.
Sheldrick, G. (2008). *SADABS*, Version 2008/1. University of Göttingen, Germany.
Spek, A. L. (2003). *J. Appl. Cryst.* **36**, 7–13.
Sysko, R. J. & Allen, D. J. M. (1993). US Patent 5248699.
Tateiwa, N. & Haga, Y. (2009). *Rev. Sci. Instrum.* p. 80.
Tumanov, N. A., Boldyreva, E. V., Kolesov, B. A., Kurnosov, A. V. & Quesada Cabrera, R. (2010). *Acta Cryst.* B**66**, 458–471.
Turillazzi, E., Riezzo, I., Neri, M., Bello, S. & Fineschi, V. (2010). *Curr. Pharm. Biotechnol.* **11**, 500–509.
Verschraagen, M., Maes, A., Ruiter, B., Bosman, I. J., Smink, B. E. & Lusthof, K. J. (2007). *Forensic Sci. Int.* **170**, 163–170.
Wei, C., Rosso, V. W. & Gao, Q. (2010). US Patent 8815894 B2.
Wood, P. A., McKinnon, J. J., Parsons, S., Pidcock, E. & Spackman, M. A. (2008). *CrystEngComm*, **10**, 368–376.
Zapata-Torres, G., Cassels, B. K., Parra-Mouchet, J., Mascarenhas, Y. P., Ellena, J. & De Araujo, A. S. (2008). *J. Mol. Graphics Modell.* **26**, 1296–1305.